

Spin Susceptibility of an Ultra-Low-Density Two-Dimensional Electron System

J. Zhu,¹ H. L. Stormer,^{1,2,3} L. N. Pfeiffer,³ K. W. Baldwin,³ and K. W. West³

¹*Department of Physics, Columbia University, New York, New York 10027*

²*Department of Applied Physics and Applied Mathematics, Columbia University, New York, New York 10027*

³*Bell Labs, Lucent Technologies, Murray Hill, New Jersey 07974*

(Received 3 October 2002; published 7 February 2003)

We determine the spin susceptibility in a two-dimensional electron system in GaAs/AlGaAs over a wide range of low densities from $2 \times 10^9 \text{ cm}^{-2}$ to $4 \times 10^{10} \text{ cm}^{-2}$. Our data can be fitted to an equation that describes the density dependence as well as the polarization dependence of the spin susceptibility. It can account for the anomalous g factors reported recently in GaAs electron and hole systems. The paramagnetic spin susceptibility increases with decreasing density as expected from theoretical calculations.

DOI: 10.1103/PhysRevLett.90.056805

PACS numbers: 73.40.-c, 71.27.+a, 71.30.+h

The low-density ground state of a degenerate electron system is one of the oldest questions of many particle physics. In two dimensions, it is expected that, in the dilute limit, the electron Fermi liquid undergoes a phase transition to a solid known as the Wigner crystal [1–3]. Furthermore, driven by the exchange coupling between electrons, a ferromagnetic state may arise at densities slightly above the critical density of Wigner crystallization [4–7]. None of these phases have yet been detected due to the lack of sufficiently high-quality, low-density specimens. Recent measurements of relevant system parameters such as the spin susceptibility χ and the effective g factor g^* have shown considerable deviations from their standard, noninteracting values [8–12]. This is believed to be the result of strong interaction [6,7,13], but disorder-led enhancement cannot be ruled out. Such explorations of the pretransition regime provide valuable data against which to check the same theoretical calculations that determine the transition point to either a ferromagnetic state or to the Wigner solid. A possible connection between the ferromagnetic properties and the metal-to-insulator transition (MIT) in low-density two-dimensional electron systems (2DES) has added to the complexity of the problem and prompted intense recent studies on this subject in silicon metal-oxide-semiconductor field-effect transistors (MOSFET) [9,10,14–16]. These results generally lend support to the possibility of a ferromagnetic state. On the other hand, two groups have recently reported anomalous density dependencies of the g factors in the GaAs/AlGaAs electron and hole systems that are at odds with results in silicon MOSFET and disfavor the predicted ferromagnetic transition [11,12].

In this paper, we report measurements of χ in a variable density 2DES of exceedingly high quality to unprecedented low densities. In addition to the density dependence of χ , our measurements determine, for the first time, the explicit polarization dependence of χ . This polarization dependence can account for the “anoma-

lous” g factors recently reported in GaAs 2DES and 2D hole systems (2DHG) [11,12].

Our specimen is a heterojunction-insulated gate field-effect transistor (HIGFET). The specimen consists of a (001) GaAs substrate, overgrown by molecular beam epitaxy with $0.5 \mu\text{m}$ of GaAs, followed by a 200-fold superlattice of 10 nm of GaAs and 3 nm of $\text{Al}_{0.32}\text{Ga}_{0.68}\text{As}$. Subsequently, $2 \mu\text{m}$ of GaAs are deposited as a channel, followed by 600 nm of $\text{Al}_{0.32}\text{Ga}_{0.68}\text{As}$ as an effective insulator, and capped by a heavily doped GaAs n^+ layer, serving as a top gate. The specimen is processed into a $600 \mu\text{m}$ square mesa. Sixteen Ni-Ge-Au contact pads are spaced evenly along the edges of the mesa using standard photolithography. One corner pad contacts the top gate, which allows for a continuous and *in situ* change of the 2DES density. The density range available for measurement extends from $1.7 \times 10^9 \text{ cm}^{-2}$ to $6.4 \times 10^{10} \text{ cm}^{-2}$. The interaction parameter r_s , defined as the ratio of the interelectron spacing to the Bohr radius, $a/a_B = 1/\sqrt{\pi n a_B}$, spans $2.2 < r_s < 13.4$. Screening of the e - e interaction via the top metallic gate can be neglected, since its distance exceeds the electron spacing by a factor of 4.4 to 27 in our experiments. The MIT occurs at $2 \times 10^9 \text{ cm}^{-2}$, which is the lowest transition density ever reported in a 2D system, attesting to the low disorder of the specimen. Our FET gives us the unique advantage of wide density tunability within one specimen and its reproducible gate-voltage/density relation lets us sweep density at fixed magnetic field, which is an essential method in our χ determination.

Our measurements were performed in a dilution refrigerator equipped with a rotating sample holder reaching a base temperature of 30 mK. A standard low frequency (3–23 Hz) lock-in technique was used with excitation currents ranging from 100 pA to 100 nA. All experiments were performed during one cooldown, facilitating quantitative comparison between our data.

In a normal Fermi liquid, the spin susceptibility $\chi = d\Delta n/dB = g^* \mu_B \rho / 2$, where g^* is the effective g factor,

ρ is the density of states at the Fermi level, and $\Delta n = n^\uparrow - n^\downarrow$. In a 2D system, $\rho = m^*/\pi\hbar^2$, therefore $\chi = g^*m^*\mu_B/2\pi\hbar^2$. Generally, theories find that χ increases with growing interaction due to spin-exchange coupling. To investigate the experimental situation, we measure the spin susceptibility χ as a function of the 2DES density n . We express it as a relative spin susceptibility $\chi/\chi_0 = m^*g^*/m_bg_b$, where $m_b = 0.067m_e$ and $g_b = 0.44$ are the band values of mass and g factor in GaAs, and χ_0 the Pauli susceptibility determined by these band values. In the remainder of the paper, we use values for χ and m^*g^* normalized to χ_0 and m_bg_b , respectively, so that $\chi = m^*g^*$. We employ two different methods to measure m^*g^* . First, we follow and extend the tilted-field method introduced by Fang and Stiles in silicon MOSFET [17]. Second, we follow the parallel-field method recently utilized by Refs. [11,12] to derive m^*g^* from the full polarization condition of the 2DES.

In a magnetic field, spin-up and spin-down electrons form two separate sets of Landau levels. As the magnetic field is tilted, the two sets of Landau levels move with respect to each other. The energy diagrams are schematically shown as insets in Fig. 1(a). Solid and dotted lines represent spin-up and spin-down Landau levels, respectively. The spacing between Landau levels, $\hbar\omega_c = e\hbar B_{\text{perp}}/m^*$, depends on the perpendicular component of the field. The shift between both sets, on the other hand, is the Zeeman energy, $\Delta E_z = g^*\mu_B B_{\text{tot}}$, which depends on the total field. By adjusting the tilt angle, θ , and the total field, B_{tot} , $\hbar\omega_c$ and ΔE_z can be independently changed. Particularly useful configurations arise when $g^*\mu_B B_{\text{tot}} = i\hbar\omega_c$, where i is an integer or a half-integer. At half-integer configurations, the Landau levels from both spins interleave and form a set of uniformly spaced levels. At integer configurations, the Landau levels coincide and form again a set of uniformly spaced levels, however, this time with double spacing compared to the half-integer case [see insets of Fig. 1(a)].

The magnetoresistance of the 2DES reflects the configuration of the energy levels. Distinctive signatures from different configurations are observed when the 2DES density is swept at fixed B_{tot} and θ . B_{perp} , and hence θ , is accurately determined from the period of the oscillations and the Landau level degeneracy eB_{perp}/h . At half-integer configurations, the depths of successive minima are just equal. This is also the case for the integer configurations, but here each second minimum disappears. The different configurations are realized only transiently at particular densities n_0 that satisfy $g^*\mu_B B_{\text{tot}} = i\hbar\omega_c$, equivalent to $m^*g^*(n_0) = ie\hbar\cos\theta/\mu_B$, since m^*g^* depends on density. Integer configurations are easily identified by the disappearance of a minimum. At half-integer configurations, the depth of neighboring minima interchange strength at n_0 , which is identified by the crossing point of two smooth envelopes drawn along alternate minima [see Fig. 1(a) for 85.71°]. The trace at 88.40° of Fig. 1(a) shows, as examples, several configurations of

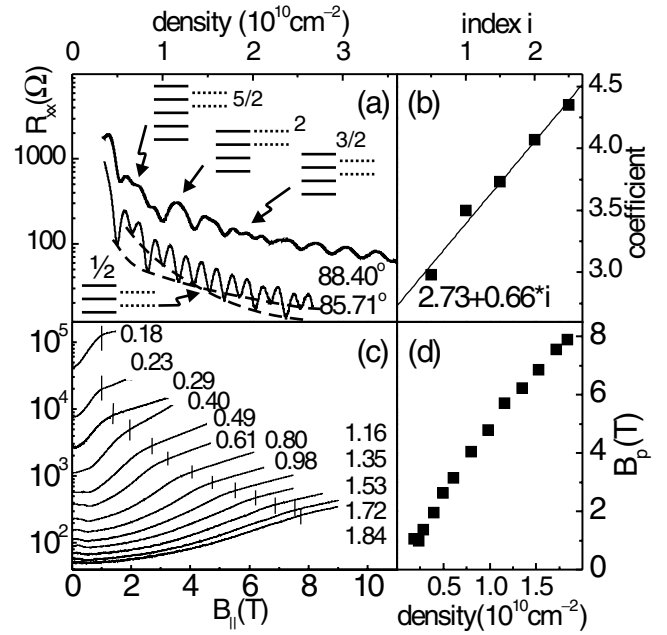


FIG. 1. (a) Density sweeps at $B_{\text{perp}} = 0.07$ T and $\theta = 85.71^\circ$ (thin line) and 88.40° (thick line), respectively. Events corresponding to $g^*\mu_B B_{\text{tot}} = i\hbar\omega_c$ where $i = 1/2, 3/2, 2$, and $5/2$ are indicated in the plot with level diagrams nearby as insets. Dashed lines illustrate the procedure to determine n_0 at half-integer configurations. (b) Linear dependence of coefficients of the power law fits of Fig. 2 on their index, i . (c) Magnetoresistances in parallel-field method for different densities in units of 10^{10} cm^{-2} . Positions of full polarization fields, B_p , are indicated following Ref. [11]. (d) B_p as a function of density.

higher indices as the density is swept and indicated by the neighboring diagrams. Increasing θ slowly and tracking the indices carefully, we are able to identify and label events that belong to configurations with index $1/2, 1, 3/2, 2$, and $5/2$. The product m^*g^* is calculated according to $m^*g^* = ie\hbar\cos\theta/\mu_B$. The solid symbols in Fig. 2 represent data derived with this method, using different symbols for different indices.

Clearly, m^*g^* increases with decreasing density and increasing index i . More strikingly, for each fixed index i , m^*g^* displays a power law dependence on n within the measured range, indicated by the dashed lines on a log-log scale. This dependence is best developed for $i = 1/2$ and $3/2$. Furthermore, the parallel lines suggest a single exponent. We therefore fit a power law dependence to the data of $i = 1/2$ and use the exponent as a constraint in fitting data of the other indices. The coefficients from these five fits display a very good linear dependence on i , as seen in Fig. 1(b). This gives us an empirical equation, $m^*g^* = (2.73 + 0.66i)n^{-0.4}$, where n is in units of 10^{10} cm^{-2} . This equation describes all our data points remarkably well.

Before discussing the implications of such an empirical equation, we proceed with the second method of determining m^*g^* . With increasing in-plane

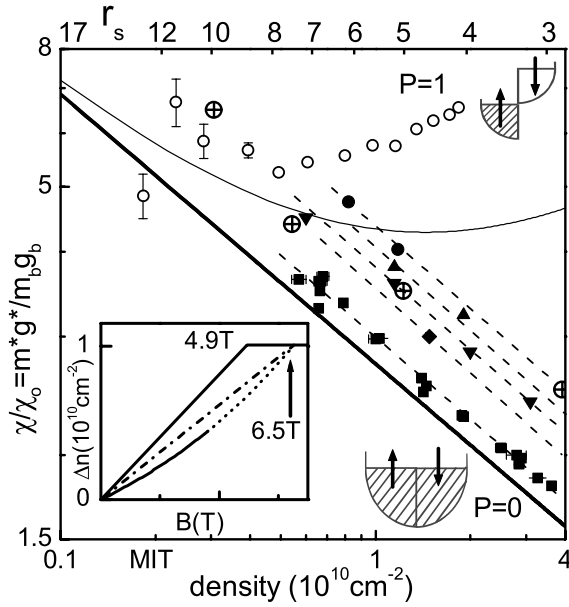


FIG. 2. Density dependence of m^*g^* determined by two different methods. Solid data points are from tilted-field experiment with different indices: square for $i = 1/2$, diamond for $i = 1$, down triangle for $i = 3/2$, up triangle for $i = 2$, circle for $i = 5/2$. Parallel dashed lines indicate power law dependence of m^*g^* with a single exponent for all i . Their coefficients depend linearly on i [see Fig. 1(b)]. Open circles show nonmonotonic density dependence of m^*g^* derived from full polarization field, B_p , of in-plane field method. The inset shows net spin $\Delta n = Pn$ for $n = 1 \times 10^{10} \text{ cm}^{-2}$ with interpolated regime (solid line) and extrapolated regime (dotted line). $B_p = 4.9 \text{ T}$ from in-plane field method and $B_{\text{ext}} = 6.5 \text{ T}$ from extrapolation of tilted-field method. A nominal $m^*g^*_{\text{ext}}$ slope of the dash-dotted line is derived from B_{ext} for all densities and plotted as a thin solid line in full figure. The thick solid line represents extrapolation of m^*g^* to the $P = 0$ limit. Calculations from Ref. [7] are shown as crossed circles.

magnetic field, B_{\parallel} , the polarization, $P = (n^{\uparrow} - n^{\downarrow})/n$ of the 2DES increases and saturates at unity at a threshold field B_p when $g^*\mu_B B_p/2 = E_F$. The derivative of $\Delta n (= Pn)$ with respect to B_{\parallel} is $\chi (= m^*g^*)$. Assuming m^*g^* to be independent of P , it follows that $m^*g^* = 2\pi\hbar^2 n/\mu_B B_p$. As asserted by several groups, full polarization of the 2DES is signaled by the onset of an exponential behavior in the parallel-field magnetoresistance [8,18–21]. We have performed such experiments on our HIGFET for different densities [Fig. 1(c)], determined B_p according to Ref. [11], and show their values in Fig. 1(d). Within experimental error, B_p is independent of the current direction relative to B_{\parallel} . Translated into m^*g^* , the results are plotted as open circles in Fig. 2. Unlike the solid data points from the first determination of m^*g^* , these new data exhibit a nonmonotonic dependence on density and are consistently larger in value than the solid data points, with the discrepancy increasing with increasing density.

The key to reconciling the discrepancy between these data sets is to recognize the dependence of m^*g^*

on the polarization, P . In the tilted-field method, a higher index i implies a higher Zeeman energy and therefore a higher degree of 2DES polarization. In the Fermi liquid limit ($B_{\text{perp}} = 0$), $P = (n^{\uparrow} - n^{\downarrow})/n = \Delta E_z \rho / 2n = (g^*\mu_B B_{\text{tot}})(m^*/2\pi\hbar^2)/n$. The tilted-field method assumes that the introduction of a small B_{perp} does not alter the values of g^* and m^* . Using the relation $g^*\mu_B B_{\text{tot}} = i\hbar\omega_c$, a straightforward calculation yields $P = ieB_{\text{perp}}/nh$. This direct relationship between P and index i establishes an explicit P dependence of m^*g^* . Substituting P for i and using $B_{\text{perp}} = 0.07 \text{ T}$ [22], we obtain $\chi = m^*g^* = (2.73 + 3.9Pn)n^{-0.4}$ from our data. Most remarkably, for fixed density n , the susceptibility χ increases linearly with increasing polarization. This monotonic increase reflects an increasing spin-exchange energy with increasing population of like spins.

Quite clearly, the assumption of a P -independent χ , assumed in Refs. [11,12] to derive m^*g^* from B_p , does not apply. Our empirical interpolation equation can be used to make contact between the data obtained from the tilted-field method and from the parallel-field method. Their relationship is best discussed referring to the inset of Fig. 2. This diagram shows, as an example, the evolution of the net spin $\Delta n = Pn = n^{\uparrow} - n^{\downarrow}$ with B_{tot} for a fixed density, $n = 1 \times 10^{10} \text{ cm}^{-2}$. By definition, the slope of $\Delta n(B)$ is the susceptibility $\chi = m^*g^*$. The parallel-field method determines $\Delta n = n (= 1 \times 10^{10} \text{ cm}^{-2})$ at $B_p = 4.9 \text{ T}$. The assumption of a B -independent m^*g^* implies a linear rise of Δn with B , shown as a straight line in the inset. One value, $B_p = 4.9 \text{ T}$, determines $m^*g^*_p = 2\pi\hbar^2 n/\mu_B B_p = 5.7$. However, the relationship between Δn and B is not linear but must be deduced from the tilted-field experiments. We derive the actual Δn vs B curve by integrating the empirical equation of $\chi(P)$ and obtain $\Delta n = 0.69[\exp(0.138Bn^{-0.4}) - 1]$. The curve for $n = 1 \times 10^{10} \text{ cm}^{-2}$ is also shown in the inset. The solid portion represents the interpolated regime of χ while the dotted portion represents extrapolation of χ beyond our tilted-field data. Requiring $\Delta n = n (= 1 \times 10^{10} \text{ cm}^{-2})$, we obtain $B_{\text{ext}} = 6.5 \text{ T}$ for the full polarization field, which is 33% higher than the measured value of B_p . This B_{ext} yields a “nominal” $m^*g^*_{\text{ext}} = 2\pi\hbar^2 n/\mu_B B_{\text{ext}} = 4.3$, equivalent to the slope of the dash-dotted line in the inset.

Performing this derivation for all densities using the interpolation equation, we arrive at an $m^*g^*_{\text{ext}}$, which is plotted as a thin, curved line in Fig. 2. It shows a qualitative similarity to the $m^*g^*_p$ data derived from the parallel-field measurements, particularly the nonmonotonic density dependence. In fact, in the low-density limit our derived curve matches $m^*g^*_p$ very well, indicating that our empirical equation extrapolates well into this regime. At higher densities considerable discrepancies arise, which one may, at first glance, attribute to a discontinuity in Δn on the polarization curve, indicating the existence of a first order phase transition. However, given the good agreement between $m^*g^*_p$ and $m^*g^*_{\text{ext}}$ at low

densities, and, hence, the absence of a phase transition in this regime, it is unlikely that such a transition occurs at higher densities. Instead, we suspect that the extrapolation of our empirical equation becomes less accurate with increasing density due to the increasing range of extrapolation and the solid curve of the inset bends sharply, but continuously towards $B = 4.9$ T. A mass increase in an in-plane field could provide a mechanism for such an accelerated bending. This effect is negligible at low field and, hence, low density, but increases rapidly with B_{\parallel} [23,24]. Alternatively, at high polarization, terms of higher order in Δn may increasingly contribute to χ , leading to an accelerated bending as well. In spite of this discrepancy for extrapolations at high densities, the qualitative and partially quantitative agreement between $m^*g^*_{ext}$ and $m^*g^*_p$ strongly suggests that our empirical equation captures correctly the underlying physics of the system.

Our analysis of m^*g^* provides a simple interpretation of the nonmonotonic behavior of m^*g^* derived from the parallel-field data. The unusual density dependence of $m^*g^*_p$ results from a combination of the polarization and density dependence of χ . Clearly, this m^*g^* does *not* reflect the actual susceptibility at any polarization value and, consequently, its density dependence cannot be used to assess the possibility of a ferromagnetic transition. By comparing measurement and extrapolation, we conclude that a first order transition is unlikely to occur in our 2DES within the regime of r_s studied (3–12.4). In the remainder of the paper, we examine χ in the limit of vanishing polarization, which plays a central role in the context of a second order ferromagnetic transition.

Our empirical formula $\chi = m^*g^* = (2.73 + 3.9Pn)n^{-0.4}$, is readily extrapolated to $P = 0$ to yield the spin susceptibility, χ , of a normal Fermi liquid (see Fig. 2). From $n = 5 \times 10^9 \text{ cm}^{-2}$ to $4 \times 10^{10} \text{ cm}^{-2}$, $\chi = 2.73n^{-0.4}$ showing an enhancement factor of 1.6 to 3.6. This extrapolation is very reliable since it extends only slightly beyond the range of our data. Furthermore, from the excellent agreement at low densities between the $m^*g^*_p$ data and the extrapolated $m^*g^*_{ext}$, we are confident that it provides very good estimates for χ to densities as low as the MIT density $n = 2 \times 10^9 \text{ cm}^{-2}$ ($r_s = 12.4$), where χ reaches about 5.5. Whether a divergence occurs at yet lower density cannot be inferred from our data.

Recent quantum Monte Carlo (QMC) calculations have predicted a weakly first order ferromagnetic transition at $r_s = 20$ –30, corresponding to $(3.4$ – $7.6) \times 10^8 \text{ cm}^{-2}$ in our 2DES [6,7]. This density range is currently beyond our reach. However, our measurement of χ as the 2DES approaches the phase transition can be compared to theory, thereby providing guidance as to the general applicability of the theoretical approach. In Fig. 2, the results of Ref. [7] are plotted as large, crossed circles. The general trend of increasing χ with increasing r_s agrees very well with our data although their estimates of χ

seem to be offset to slightly larger values compared to experiment.

In conclusion, we have determined the polarization and density dependence of the enhanced spin susceptibility $\chi \sim m^*g^*$ in a 2DES in GaAs/AlGaAs over a wide range of low densities. Our analysis provides an explanation for the anomalous g factors reported recently in GaAs 2DES and 2DHG. The susceptibility χ of the paramagnetic Fermi liquid increases with decreasing density, in qualitative agreement with recent QMC calculations.

We thank D.C. Tsui for inspiring discussions and A. Millis for many insightful suggestions. Financial support from the W.M. Keck Foundation is gratefully acknowledged.

-
- [1] E. Wigner, Phys. Rev. **46**, 1002 (1934).
 - [2] A.V. Chaplik, Sov. Phys. JETP **35**, 395 (1972).
 - [3] B. Tanatar and D.M. Ceperley, Phys. Rev. B **39**, 5005 (1989).
 - [4] F. Bloch, Z. Phys. **57**, 545 (1929).
 - [5] E.C. Stoner, Proc. R. Soc. London A **165**, 372 (1938).
 - [6] D. Varsano, S. Moroni, and G. Senatore, Europhys. Lett. **53**, 348 (2001).
 - [7] C. Attaccalite, S. Moroni, P. Gori-Giorgi, and G.B. Bachelet, Phys. Rev. Lett. **88**, 256601 (2002).
 - [8] T. Okamoto, K. Hosoya, S. Kawaji, and A. Yagi, Phys. Rev. Lett. **82**, 3875 (1999).
 - [9] A.A. Shashkin, S.V. Kravchenko, V.T. Dolgoplov, and T.M. Klapwijk, Phys. Rev. Lett. **87**, 086801 (2001).
 - [10] V.M. Pudalov, M.E. Gershenson, H. Kojima, N. Butch, E.M. Dizhur, G. Brunthaler, A. Prinz, and G. Bauer, Phys. Rev. Lett. **88**, 196404 (2002).
 - [11] E. Tutuc, S. Melinte, and M. Shayegan, Phys. Rev. Lett. **88**, 036805 (2002).
 - [12] H. Noh, M.P. Lilly, D.C. Tsui, J.A. Simmons, L.N. Pfeiffer, and K.W. West, cond-mat/0206519.
 - [13] S. Yarlagadda and G.F. Giuliani, Phys. Rev. B **40**, 5432 (1989).
 - [14] For a review of the MIT, see E. Abrahams, S.V. Kravchenko, and M.P. Sarachik, Rev. Mod. Phys. **73**, 251 (2001).
 - [15] S.A. Vitkalov, H. Zheng, K.M. Mertes, M.P. Sarachik, and T.M. Klapwijk, Phys. Rev. Lett. **87**, 086401 (2001).
 - [16] A.A. Shashkin, S.V. Kravchenko, V.T. Dolgoplov, and T.M. Klapwijk, Phys. Rev. B **66**, 073303 (2002).
 - [17] F.F. Fang and P.J. Stiles, Phys. Rev. **174**, 823 (1968).
 - [18] S.A. Vitkalov, H. Zheng, K.M. Mertes, M.P. Sarachik, and T.M. Klapwijk, Phys. Rev. Lett. **85**, 2164 (2000).
 - [19] V.T. Dolgoplov and A. Gold, JETP Lett. **71**, 27 (2000).
 - [20] E. Tutuc, E.P.D. Pootere, S.J. Papadakis, and M. Shayegan, Phys. Rev. Lett. **86**, 2858 (2001).
 - [21] I.F. Herbut, Phys. Rev. B **63**, 113102 (2001).
 - [22] For $i = 1, 3/2, 2, 5/2$, all B_{perp} is within 10% of 0.07 T. Data taken for $i = 1/2$ at $B_{\text{perp}} \sim 0.07$ T and $B_{\text{perp}} \sim 0.05$ T are identical within experimental errors.
 - [23] E. Batke and C.W. Tu, Phys. Rev. B **34**, 3027 (1986).
 - [24] S. Oelting, A.D. Wieck, E. Batke, and U. Merkt, Surf. Sci. **196**, 273 (1988).